Bioresource Technology 361 (2022) 127701

Contents lists available at ScienceDirect

Bioresource Technology

journal homepage: www.elsevier.com/locate/biortech

Effect of pressure on biomethanation process and spatial stratification of microbial communities in trickle bed reactors under decreasing gas retention time

Farinaz Ebrahimian [a,b,1], Nicola De Bernardini [c,1], Panagiotis Tsapekos [a,*], Laura Treu [c], Xinyu Zhu [d], Stefano Campanaro [c], Keikhosro Karimi [b,e], Irini Angelidaki [a]

[a] Department of Chemical and Biochemical Engineering, Technical University of Denmark, Kgs. Lyngby DK-2800, Denmark
[b] Department of Chemical Engineering, Isfahan University of Technology, Isfahan 84156-83111, Iran
[c] Department of Biology, University of Padova, Via U. Bassi 58/b, 35121 Padova, Italy
[d] School of Engineering, Westlake University, No.18, Shilongshan Road, Cloud Town, Xihu District, Hangzhou, Zhejiang Province, China
[e] Department of Chemical Engineering, Vrije Universiteit Brussel, 1050 Brussels, Belgium

HIGHLIGHTS

- Elevated pressure led to efficient biomethanation at gas retention time of 21 min.
- The elevated pressure did not significantly affect the microbial composition.
- *Methanobacterium* DTU-pt_142 was the dominant hydrogenotrophic methanogenic archaeon.
- Distribution of *Methanobacterium* DTU-pt_142 became more uniform at high feed rate.

GRAPHICAL ABSTRACT

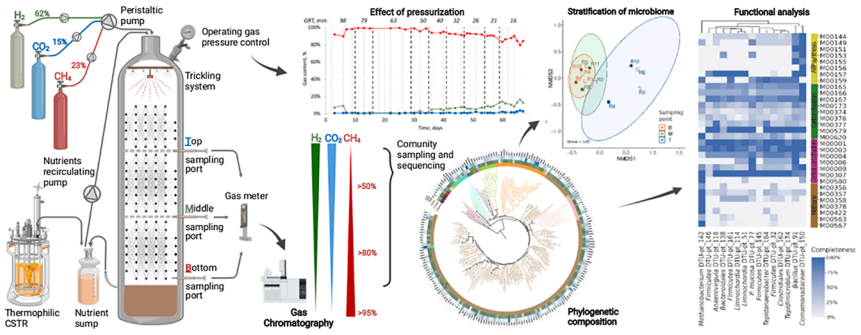

ARTICLE INFO

Keywords:
Biogas upgrading
Ex-situ
Metagenomic analysis
Biofilm
Power-to-gas

ABSTRACT

The current study investigated the effect of elevating gas pressure on biomethanation in trickle-bed reactors (TBRs). The increased pressure led to successful biomethanation (CH_4 > 90 %) at a gas retention time (GRT) of 21 min, due to the improved transfer rates of H_2 and CO_2. On the contrary, the non-pressurized TBR performance was reduced at GRTs shorter than 40 min. Metagenomic analysis revealed that the microbial populations collected from the lower and middle parts of the reactor under the same GRT were more homogeneous compared with those developed in the upper layer. Comparison with previous experiments suggest that microbial stratification is mainly driven by the nutrient provision strategy. *Methanobacterium* species was the most dominant methanogen and it was mainly associated with the bottom and middle parts of TBRs. Overall, the increased pressure did not affect markedly the microbial composition, while the GRT was the most important parameter shaping the microbiomes.

* Corresponding author at: Department of Chemical and Biochemical Engineering, Technical University of Denmark, Bld 228A, 2800 Lyngby, Denmark.
E-mail address: ptsa@kt.dtu.dk (P. Tsapekos).
[1] These authors have contributed equally to this work.

https://doi.org/10.1016/j.biortech.2022.127701
Received 1 June 2022; Received in revised form 20 July 2022; Accepted 22 July 2022
Available online 26 July 2022

1. Introduction

The main challenge in microbial biogas upgrading is the low H_2 gas–liquid mass transfer, which restricts its availability for methane producing microorganisms. Thus, the enhancement of H_2 transfer into the liquid phase is essential for maximizing the conversion efficiency to CH_4 and therefore increasing the production capacity of the biomethanation process (Dupnock & Deshusses, 2021).

Ex-situ biogas upgrading - carried out by injecting the biogas together with hydrogen in a separate reactor after the first biomethanation phase - offers a more flexible operation compared to in-situ process (Sieborg et al., 2020). A wide variety of bioreactor configurations have been employed on ex-situ biomethanation to enhance H_2 accessibility, including membrane bioreactor, bubble column, up-flow column, trickle bed reactor (TBR), and continuously stirred tank. Among these, TBR has been reported to lead a superior gas liquid mass transfer along with low energy requirements and low operating costs (Asimakopoulos et al., 2020). The higher H_2 and CO_2 availability in TBRs is associated with the direct contact between the gas phase and a microbial community with large surface-area (Jønson et al., 2020), which is achieved through the formation of biofilm on top of the packing material in the reactor (Kougias et al., 2020). Until today the biocatalyzer tested in TBR systems divides into: pure microbial community, composed of a single hydrogenotrophic archaeal species; and mixed culture, formed by a subset of the native microbiome involved in the natural methanation process (Thema et al., 2021). The setup of TBR using a single autotrophic methanogen has the advantage of excluding the microbial variability, thus allowing better investigation of the operational parameters affecting carbon fixation. Nevertheless, aiming at the implementation of this technology at industrial scale, the number of requirements to maintain sterile conditions for pure cultures are extremely demanding. Not only, single microbe community need frequent refreshing of the synthetic growth medium, species-specific supplements concentration (e.g., ammonium, hydrogen sulfide, sodium sulfide, and foam control) and pH level. In comparison, mixed culture systems provide robust behavior toward input gas purity, adapting itself to varying pH, nutrient source and operational conditions. Moreover, the design of TBRs demonstrated to favor the development of microbiomes enriched in active species important for methanogenic processes (Dupnock & Deshusses, 2017). The drift of microbial composition toward consortia of species adapted to gas feeding is essential to enhance methanation performances in upgrading reactors (Treu et al., 2018). Extensive investigation of microbial communities' adaptation in upgrading flasks reactors highlighted that the inoculum indigenous composition tends to evolve towards a more simplified but specialized H_2-utilizing microbial consortia (Braga Nan et al., 2020). This type of community composition and adaptation events took place consistently in TBRs and were observed by comparing microbiomes in the inoculum, the recirculating liquid phase, and the biofilm. Specifically, methanogenic hydrogenotrophic archaea belonging to the genera *Methanobacterium* (Braga Nan et al., 2020; Porté et al., 2019; Tsapekos et al., 2021) and *Methanothermobacter* (Kougias et al., 2020) were dominant, and bacteria, primarily members of *Firmicutes* and in minor part *Proteobacteria*, are usually enriched (Ashraf et al., 2020).

In addition to the reactor configuration, the operating pressure is a fundamental factor in the biological methanation of H_2 and CO_2 (Ullrich et al., 2018). In general, pressurized reactor features a higher gas–liquid mass transfer and increased accessibility of the reactant gases (Mauerhofer et al., 2021). It has been previously demonstrated that raising the operating pressure in a TBR can significantly enhance the conversion rate of CO_2 and H_2 and consequently increase the methane content from 64.1 % at 1.5 bar to 86.5 % at 9 bar (Ullrich et al., 2018). In another study, elevating the reactor pressure from 10 bar to 50 bar in a continuous high pressure two-stage anaerobic digestion led to an increase in methane content from 70.08 % to 90.45 % (Merkle et al., 2017). However, the application of very high pressure not only increases the operational costs but also maximizes the probability of leakage and reactor collapse (Mauerhofer et al., 2021). Thereby, although higher methane contents can be achieved, high pressure levels can present a technical challenge for biological methanation.

Pressure, along with other operational conditions, are important in biological methanation because they shape the microbial community composition, which in turn affects the overall efficiency (Tsapekos et al., 2021). Knowledge of microbial community composition, in response to working parameters, would contribute in optimizing operational conditions. The inspection of microbial communities can be performed through genome-centric metagenomics, which permits deep insights into the structure of the methanogenic consortium (Fontana et al., 2018). Furthermore, reconstruction of metabolic networks from metagenome-assembled genomes (MAGs) allows to understand the metabolic potential of individual microbes and elucidate existence of intricate interspecies microbial dynamics (Basile et al., 2020). Nevertheless, few studies have applied this effective technique to characterize microbiome in upgrading TBR (Porté et al., 2019) and, to our knowledge, none of the used experimental settings has evaluated the effect of pressurization on microbiome composition. Moreover, although pressurized biogas upgrading has numerous benefits over the conventional approach, studies on pressurized trickling bed reactor are scarce, focusing only on the effect of pressure on conversion rates and methane production capacity. However, detailed information on the effect of pressure on gas retention time, microbial dynamicity, and maximum achievable productivity through the biomethanation of H_2 and CO_2 are still missing. In particular, the state of the biological system across the axial direction of the reactor as a consequence of changes in process operation (e.g., increasing pressure or feeding rate) have not been clearly elucidated. Tsapekos et al. (2021) explored the microbial species stratification across the height of the reactor highlighting a clear gradient. The hydrogenotrophic archaea were enriched in the layers closer to the gas source, thus where the concentration of H_2 and CO_2 was the highest and the methanation is thermodynamically favored (Garcia-Robledo et al., 2016). Nevertheless, the hypothesis that proximity to the gas is the main driver shaping the community microbial stratification at large scale (i.e., across a pilot reactor) is not confirmed. The previous experimental settings did not assess whether the co-current or counter-current flow of gas and digestate can affect the microbial composition in a well-performing TBR. In another study, Dupnock and Deshusses (2017) analyzed the vitality of cells at different heights in a TBR but did not quantify how the microbial stratification contributes to the CO_2 to CH_4 conversion across the reactor. Finally, the reduction of GRT often demonstrates drops in methanation performances but microbiomes have not been characterized yet to identify how this process parameter drives shifts in the community composition (Tsapekos et al., 2021).

The main objective of the present study is to assess the effect of pressure on TBR performance. Two TBRs under pressurized and non-pressurized conditions were developed for biomethanation of H_2 and CO_2. Gas retention time (GRT) was progressively reduced by increasing the inlet flowrate of feed gases to investigate the stability and production capacity of the process at the minimum achievable GRT. Moreover, the initial inoculum and biofilm samples taken from three different sampling ports over the TBRs height, as top, middle, and bottom, at short and long GRTs were subjected to metagenomic analysis to clarify the role of microbial community in the upgrading process.

2. Materials and methods

2.1. Setup and monitoring of the trickling bed reactors

The TBRs were made of glass column with a height of 51 cm and a packed working volume of 0.8 L. The TBRs were filled with polyethylene Raschig rings (PE08, Tongxiang Small Boss Special Plastic Products ltd) and each piece had a dimensions of 7 mm × 10 mm with a surface area of

3500 m^2/m^3. The experiment was conducted under thermophilic conditions (54 ± 1 °C) at distinctly different periods based on the GRT (Table 1). The feeding gas contained 62 % H_2 and 15 % CO_2 (with stoichiometric H_2/CO_2 ratio of 4:1) as well as 23 % CH_4. The stream corresponds to the composition of the gaseous feedstock after mixing the biogas with exogenous H_2 for biological upgrading. The gas was supplied in concurrent flow with digestate collected from a manure-based continuously stirred tank reactor (CSTR) that was used as a nutrients source. The initial inlet gas flowrate was set at 14.65 $L.Lr^{-1}.day^{-1}$ using a peristaltic pump. After achieving steady CH_4 content above 90 % for 5 consecutive days, the inlet gas flowrate was increased by 25 % to proceed at the next period (i.e. inlet gas flowrate of 18.31 $L.Lr^{-1}.day^{-1}$) increasing the pump speed. For the entire experiment, the same strategy was followed to proceed to the next operational periods. The distinction between the two TBRs was the operating gas pressure. TBR1 was used as a control and operated at non-pressurized conditions through the whole experiment. On the contrary, overpressure of 0.7 bar was autogenerated in TBR2. Specifically, unlike TBR1, the generated biogas in TBR2 did not immediately leave the reactor until the pressure of 0.7 bar was achieved, using a barometer with a control valve at the outlet gas port.

The TBRs were inoculated with a thermophilic inoculum enriched in hydrogenotrophic methanogens (i.e. H_2 and CO_2 were used as the only energy and carbon source) that was obtained from a lab scale CSTR (Treu et al., 2018). The characteristics of the applied inoculum were: pH 8.6, total solids 1.80 ± 0.01 % (w/w), volatile solids 0.80 ± 0.01 % (w/w), total ammonia nitrogen (TAN) 687.01 ± 13.51 mg NH_4^+-N/L, and volatile fatty acids (VFAs) 99.01 ± 7.41 mg/L.

The digestate was pasteurized before usage and trickled at a constant flowrate of 20 $mL.Lr^{-1}.min^{-1}$. To avoid shortage of micro- and macronutrients, 100 mL of digestate was replaced from the sump with manure-based digestate (Period 1–5: every 4 days; Period 6–9: every 2 days). Moreover, the TBRs were flooded with the liquid volume from the sump twice per week to further ensure wetting of packing materials and access of methanogenic microbes to the nutrients.

2.2. Analytical methods

The total outlet gas was measured by means of a water displacement gas-counting system. The gas composition over the TBRs height was analyzed using a gas chromatograph (Thermo Fisher Scientific, US) equipped with a thermal conductivity detector. Liquid samples were withdrawn from the nutrient sump twice per week for the analysis of pH, TAN, and VFAs. VFAs concentrations were measured by a gas chromatograph (Thermo Fisher Scientific, US) equipped with a flame ionization detector (FID) (Tsapekos et al., 2021). Total solids, volatile solids, pH, and TAN were determined as described previously (Ghofrani-Isfahani et al., 2021). All samples were analyzed in duplicate.

Table 1
Gas retention times (GRT) and inlet gas flow rates (F_{in}) at each experimental period.

Period	GRT (min)	F_{in} ($L.Lr^{-1}.day^{-1}$)*			
		H_2	CO_2	CH_4	Total
1	98	9.08	2.20	3.37	14.65
2	79	11.35	2.75	4.21	18.31
3	63	14.19	3.43	5.26	22.89
4	50	17.74	4.29	6.58	28.61
5	40	22.17	5.36	8.23	35.76
6	32	27.72	6.71	10.28	44.70
7	26	34.65	8.38	12.85	55.88
8	21	43.31	10.48	16.07	69.85
9	16	54.13	13.10	20.08	87.31

*L_r: Volume of reactor (L).

2.3. Microbial sampling and treatment

The microbial spatial stratification through the TBR height and the effect of different GRT regimes on microbiome diversity were assessed. Three samples per reactor, one per sampling point, were collected from the top, middle, and bottom filters at different time points. The DNA extraction was performed at a GRT of 63 min (Period 3) and at the end of the experiment. Moreover, the microbiome of the inoculum (In) was characterized; thus, in total thirteen samples were analyzed. Genomic DNA extraction was performed using a modified version of the DNeasy PowerSoil® (QIAGEN GmbH, Hilden, Germany) protocol as previously described (Treu et al., 2019); an initial cleaning step with Phenol, Chloroform and Isoamyl Alcohol (25: 24: 1) was implemented to increase the purity of the extracted nucleic acids. NanoDrop (Thermo Fisher Scientific, Waltham, MA, USA) and Qubit (Thermo Fisher Scientific, Waltham, MA, USA) were respectively used for purity and concentration quality control on extracted DNA.

2.4. Metagenomic sequencing and binning analysis

The sequencing strategy was based on the NextSeq 6000 platform (Illumina Inc., San Diego CA). Library preparation was performed using Nextera DNA Flex Library Prep Kit (Illumina Inc., San Diego CA) at the CRIBI Biotechnology Center sequencing facility (University of Padova, Italy) and sequenced with Illumina NovaSeq 6000 platform (2 × 150, paired end). Raw sequences were uploaded to the Sequence Read Archive (NCBI) under the project PRJNA802325.

Initial steps of the reads processing included filtering with Trimmomatic (v0.39-1) (Bolger et al., 2014) and BBDuck tool of the BBTools suite (v38.93) (De Bernardini et al., 2022). These steps removed adapters, low-quality fragments (average Phred score ≤ 20) and bacteriophage phi x174 contamination. High-quality reads were assembled using MegaHit (v1.2.9) with "*meta*-sensitive" option and considering only contigs with a minimum length equal to 1 kbp (Li et al., 2015). Bowtie2 (v2.4.4) and SAMtools (v1.12-1) were used to generate the contigs coverage profiles needed to retrieve the Metagenome Assembled Genomes (MAGs). Five different tools were included in the binning approach: Concoct (v1.1.0), Maxbin2 (v2.2.7), MetaBAT (v1:2.15), MetaBAT2 (v2:2.15) and VAMB (v3.0.2-1) (Alneberg et al., 2014; Kang et al., 2015; Kang et al., 2019; Nissen et al., 2021; Wu et al., 2014). Quality of MAGs resulting from each binning tool were assessed using CheckM (v1.1.3-1). This characterization allowed filtering MAGs (completeness ≤ 50 %, contamination ≥ 10 %) during the de-replication step. dRep (v3.2.2) were used to aggregate MAGs when their average nucleotide identity exceeded 95 % and their overlap was at least 50 %. Finally, MAGs were classified as high, medium and low quality according to the minimum information about metagenome-assembled genome guidelines (MIMAG) (Bowers et al., 2017). Further statistics and functional analysis took into consideration only MAGs with high and medium quality. Moreover, in order to better characterize the microbial community, the recovered MAGs were compared with an updated version of the Bio-Gas microbiome reference database and the microbiome of a TBR fed with real biogas (Campanaro et al., 2020; Tsapekos et al., 2021). For these comparisons, CheckM and dRep were used as described above.

The taxonomy of MAGs was defined using GTDB-Tk (v1.7.0) (Chaumeil et al., 2020) and the resulting classification was further refined based on SILVA ACT applied to 16S rRNA sequences extracted from the MAGs (Pruesse et al., 2012). The phylogenetic tree was generated using PhyloPhlAn 3.0 (3.0.51) (Asnicar et al., 2020) and drawn with iTOL (Letunic & Bork, 2021).

2.5. Statistics and functional analysis

MAGs distribution in samples was assessed via Non-metric multidimensional scaling (NMDS) performed with the phyloseq (v1.16.2)

package in R (v4.0.4). The analysis was performed using the Bray-Curtis dissimilarity metric and the goodness of the final ordination plot was assessed through stress measure. Using the PERMANOVA test from the vegan (v2.4-2) package, the statistical significance of microbiome composition similarities between the samples were assessed. To verify the assumption of this statistical test homogeneity of groups dispersions was also tested and resulted not significant. To assess the microbial composition differences, samples have been divided into groups according, in the first case, to the operational pressure, thus comparing R1-6 with R7-12. In the second case samples were divided based on GRT, which correspond to compare R1-3,7-9 with R4-6,10-12. In the third case, they were separated according to the height of the sampling point, thus testing differences between R1,4,7,10, R2,5,8,11, and R3,6,9,12. All reported statistics and statistical tests performed in this paper excluded results associated with the inoculum, given its lack of relevance for the explanation of the observed process.

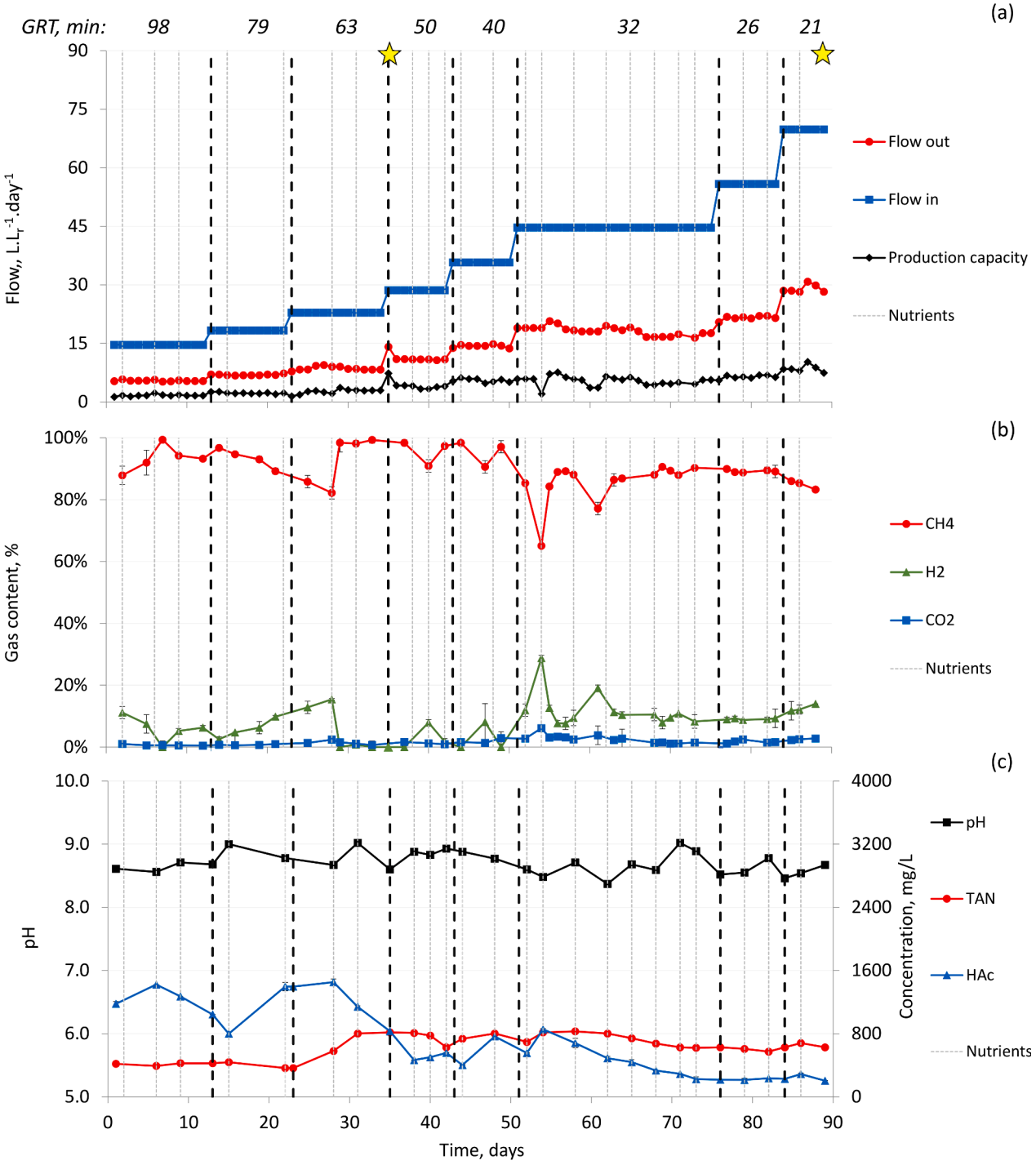

Fig. 1. Development of gas flows and production capacity (a), effluent gas composition (b), and pH, concentrations of acetic acid and total ammonium (c) using the non-pressurized reactor. The dates for DNA extraction are shown in yellow stars and the replacement of digestate in the nutrients sump are depicted in dashed lines. (For interpretation of the references to colour in this figure legend, the reader is referred to the web version of this article.)

Functional annotation, starting from ORFs prediction, was performed using Prodigal (v2.6.3) and EggNOG (v5.0.2) tools (Huerta-Cepas et al., 2019; Hyatt et al., 2010). Whereas metabolic and functional trait profiles were determined with MicrobeAnnotator (v2.0.5) (Ruiz-Perez et al., 2021). Out of the EggNOG and MicrobeAnnotator tool results, only the KEGG pathways and modules of importance for biogas production were selected and visualized as heatmap. To identify the copy number of genes associated with biofilm formation a specific list of KO were used to search EggNog results.

3. Results and discussion

3.1. Effect of pressure and increased gas feeding on biomethanation

The inlet and outlet gas flowrates, CH_4 production capacity (volume of produced CH_4 per volume of the reactor per day, $LCH4.Lr^{-1}.day^{-1}$), outlet gas composition, as well as pH value, acetic acid (the dominant VFA) concentration, and total ammonia concentration during the experimental periods of TBR1 and TBR2 are illustrated in Fig. 1 and Fig. 2, respectively.

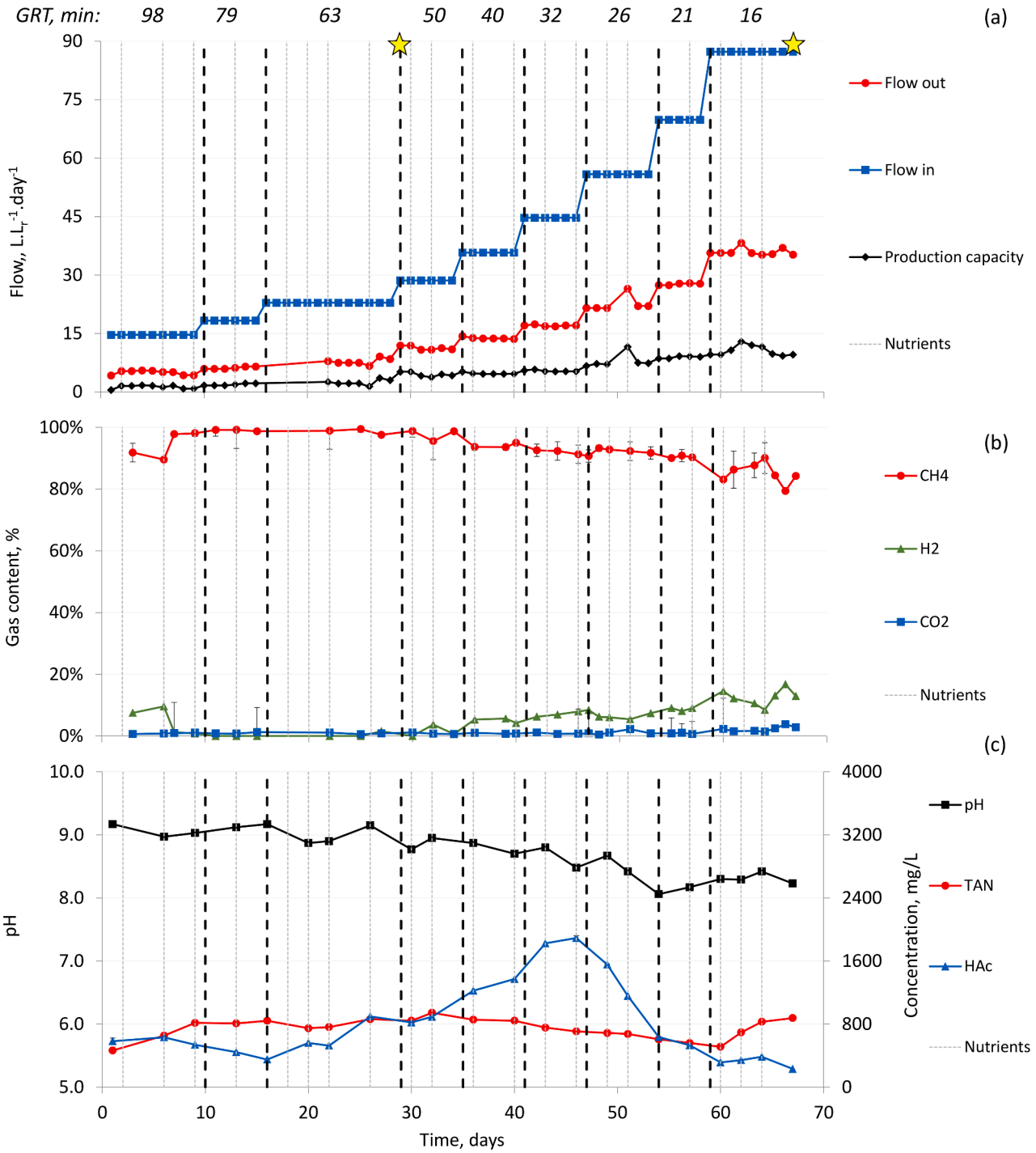

Fig. 2. Development of gas flows and production capacity (a), effluent gas composition (b), and pH, concentrations of acetic acid and total ammonium (c) using the pressurized reactor. The dates for DNA extraction are shown in yellow stars and the replacement of digestate in the nutrients sump are depicted in dashed lines. (For interpretation of the references to colour in this figure legend, the reader is referred to the web version of this article.)

The initial inlet gas flowrate was 14.6 $L.Lr^{-1}.day^{-1}$ with a GRT of 98 min. Generally, decreasing the GRT (increasing the inlet gas flowrate) increased methane production capacity in both reactors (Figs. 1, 2). This is in accordance with the higher inlet of H_2 and CO_2 which leads to higher CH_4 generation (Inkeri & Tynjälä, 2020). The main purpose of the present study was to achieve the lowest possible GRT to enhance the techno economic viability of the upgrading process for commercialization. However, shorter GRTs can lead to limited solubility and mass transfer of CO_2 and H_2 into the liquid phase which consequently limits their bioconversion into CH_4 (Sieborg et al., 2020). It has been previously reported that increasing pressure can significantly improve the in-situ biomethanation of CO_2 and H_2 as a result of enhanced gas–liquid mass transfer, leading to a H_2 conversion of 99 % during in-situ upgrading (Díaz et al., 2020). In the current study, the increased pressure affected the gas composition over the TBR height and CH_4 production capacity as well as the minimum achievable GRT for stable CH_4 content of over 90 %.

Regarding TBR1 (Fig. 1), the lowest GRT which led to a steady CH_4 content of up to 90 % was 40 min, leading to a CH_4 production capacity of 5.6 $LCH4.Lr^{-1}.day^{-1}$ with an average methane content of 95 %. A further reduction of GRT to 21 min resulted in the higher CH_4 production capacity of approximately 8 $LCH4.Lr^{-1}.day^{-1}$; however, the CH_4 quality was lowered to 85 %. This is due to the limited hydrogen-liquid mass transfer at the low GRT (high inlet gas flowrate), limiting the availability of H_2 for the methanogens (Bassani et al., 2016). Thus, the non-pressurized reactor resulted in the CH_4 contents of above 90 % only at the GRTs up to 40 min. On the contrary, in the pressurized reactor, the outlet H_2 content of lower than 10 % and CH_4 content of up to 90 % was achieved and remained such until the end of 8th period at GRT of 21 min. Thus, the increased pressure led to >90 % CH_4 even at the short GRT of 21 min, as a result of improved transfer rates of H_2 and CO_2, leading to a faster upgrading process. Comparing the CO_2 content of TBR1 with that of TBR2 under the same GRT also proved that the elevated pressure enhanced the CO_2 consumption which was associated with lower CO_2 concentration in TBR2. The results agreed with previous studies on ex-situ biomethanation carried out in pressurized biotrickling reactors (Ullrich et al., 2018) and single-culture CSTR (Martin et al., 2013). In another study Ullrich et al. (2018) reported that raising the pressure in an anaerobic filter reactor can significantly enhance the CH_4 content of biogas from 64 % at 1.5 bar to 86 % at 9 bar. However, for the high operation pressure, they reported a significant drop in pH value due to the enhanced formation of carbonic acid.

From period 5 on, the GRT reduction led to increased content of underutilized H_2 and CO_2 content in both TBRs. In parallel, acetic acid

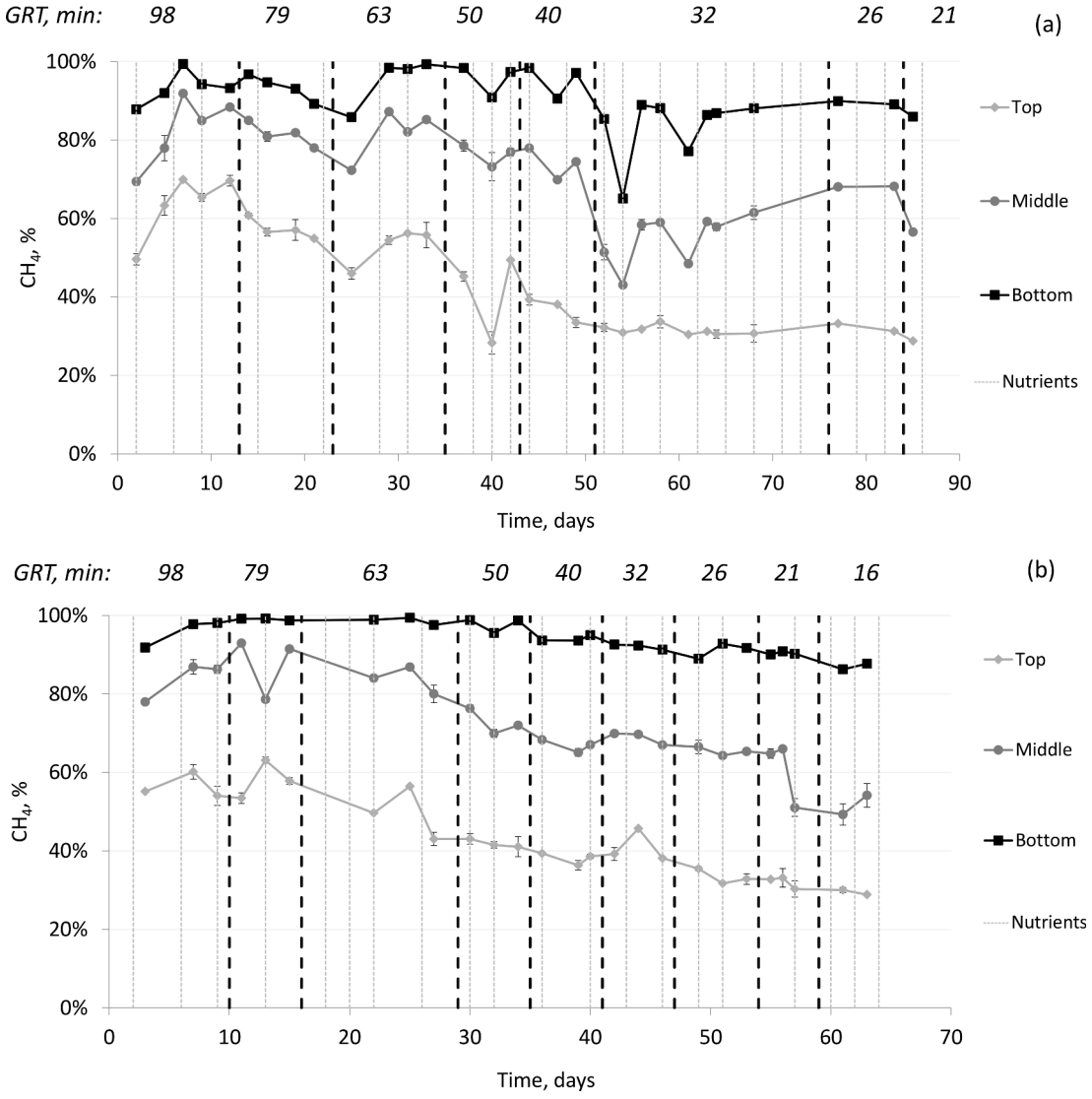

Fig. 3. CH_4 content at top, middle, and bottom part of non-pressurized (a) and pressurized (b) reactor. The dates for the replacement of digestate in the nutrients sump are depicted in dashed lines.

concentrations were decreased over time at shorter GRT indicating decreased gas consumption by both methanogenic and homo-acetogenic microorganisms due to the limited gas-to-liquid mass transfer. TBR2 had overall slightly higher acetic acid concentration and lower pH in comparison with TBR1, which can be attributed to the enhanced transfer rate of gases to the liquid phase as a consequence of the elevated pressure. Although homoacetogenesis was favored at TBR2 as more H_2/CO_2 could be available in the liquid phase, it has been demonstrated that homoacetogens require a higher H_2 content for being activated due to their higher K_s value compared to that of hydrogenotrophic methanogens (Liu et al., 2016). Additionally, homoacetogens have been demonstrated to have a lower H_2 conversion rate due to their lower maximum specific feedstock consumption rate compared to methanogens (Liu et al., 2016).

Apart from speeding up the biogas upgrading (i.e., lowering the minimum achievable GRT from 40 min to 21 min), the elevated pressure also increased CH_4 content over TBR height. For instance, as illustrated in Fig. 3(a) and (b), at period 9, the average CH_4 content at top, middle, and bottom parts of TBR2 were 41 %, 69 %, and 92 %, respectively, which were respectively higher than 29 %, 52 %, and 83 % in TBR1. This observation is of particular importance indicating that TBR height can be decreased remaining its efficiency. Then, the capital expenditures for building a full-scale TBR can be reduced and thus, improve profitability. To support the decision making, mathematical modelling can be applied to predict the relationship between the gas flow, operating pressure and TBR height. Understanding biomethanation efficiency over TBR bed can guide towards improved reactor design.

3.2. Microbiome in biogas upgrading

Analysis of microbial genomes was performed using a genome-centric metagenomic approach that generated, in total, 203 MAGs (see Supplementary Materials). The reconstructed microbial genomes accounted for the majority of the community, with the average mapped reads across all the samples being 85 % ± 2.7 %. The only exception was the inoculum with 80 % of the reads mapping of the reconstructed community. The identified MAGs belonged to 14 different phyla, two of which were candidatus taxa (Fig. 4); the most widespread phylum was *Firmicutes* (n:136) followed by *Proteobacteria* and *Tenericutes* with 23 and 11 MAGs, respectively (see Supplementary Materials). Within the community the methanogenic species were represented by four archaea: *Methanomassiliicoccaceae* DTU-pt_54, *Methanothermobacter wolfeii* DTU-pt_41, *Methanoculleus* DTU-pt_61 and *Methanobacterium* DTU-pt_142. However, only the last one appeared to play a dominant role (approx.

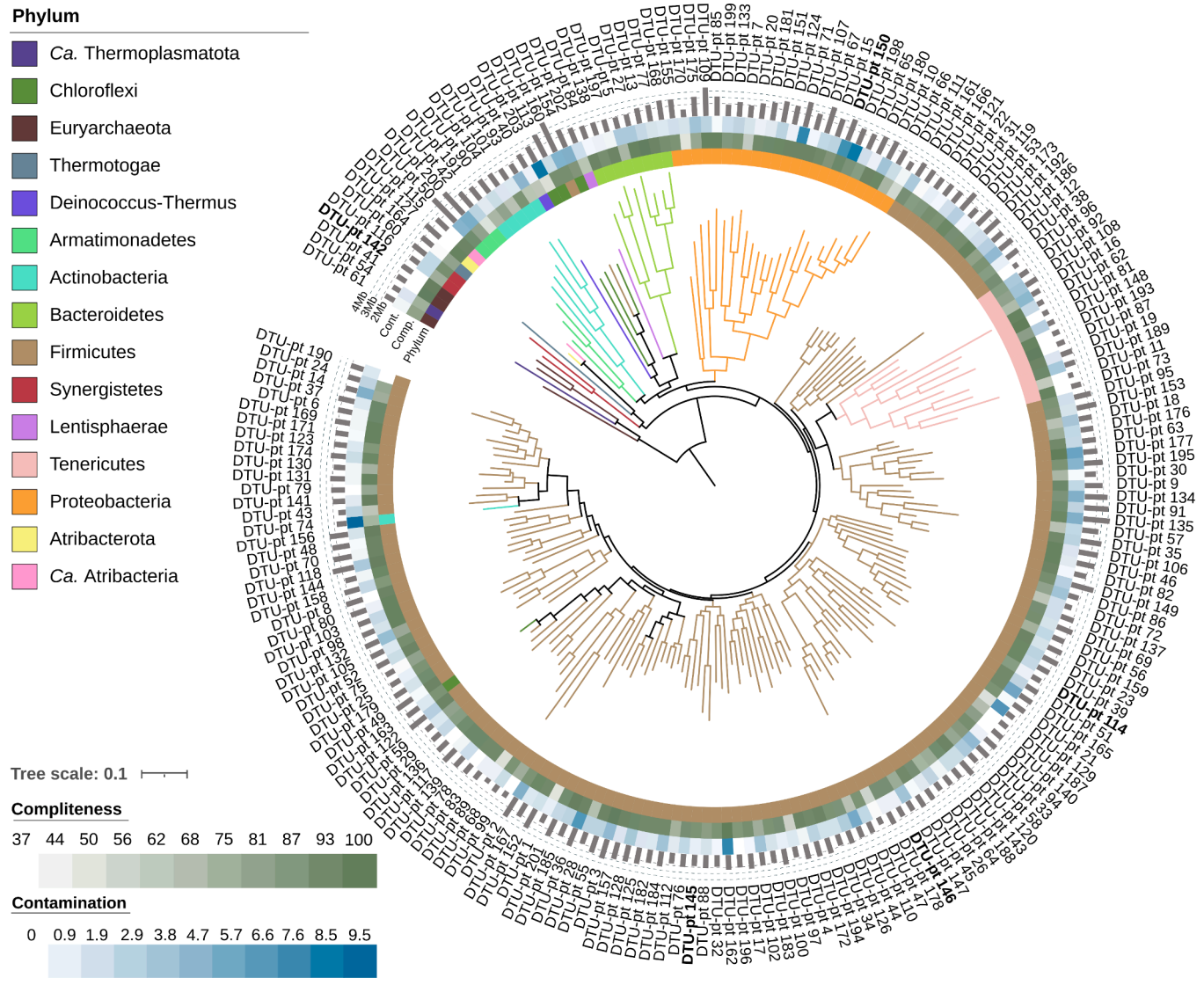

Fig. 4. Quality and phylogenetic tree of reconstructed MAGs. From outside inwards the circles indicate genome size (bar barplot), contamination, completeness and taxonomic assignment (heatmap). The phylogenetic tree was rerouted on the archaeal species and the most relevant MAGs were highlighted in bold.

relative abundance 11.7 %), whereas the other species sum up on average only to 0.32 % of the total (see Supplementary Materials).

The microbiome structure in the TBRs can be appreciated by the relative abundance and distribution of the dominant species (>1%, Fig. 5a). The populations collected from the lower and middle part of the reactor under the same GRT regime were the most homogeneous, whereas those developed in the upper layer were relatively diverse. Hierarchical clustering results confirmed this trend (Fig. 5b), highlighting a distinction between the coverage profiles and suggesting a stratification of the community. Compared to the other samples the inoculum had a clear distinct profile and clustered individually. In particular, the dominant species in the inoculum, such as Ca. *Atribacteria* DTU-pt_115 (relative abundance: 20.1 %), *Bacteroidales* DTU-pt_197 (12.5 %) and *Firmicutes* DTU-pt_140 (7.1 %), drastically decreased in abundance (<1.2 %) in the other samples. It is plausible that these species were designated to perform the most important bioprocesses in the inoculum, however the modification of the growth environment, from liquid (i.e. CSTR) to biofilm based (i.e. TBR), caused a reduction of their competitive advantages and, consequently, their abundance. The structure of the community in the TBR samples was further explored through NMDS analysis (Fig. 5c). A clear distinction between samples at different heights within the same reactor and between sampling points under different GRT regime was statistically evaluated. PERMANOVA tests were applied to the Bray-Curtis distances and confirmed statistical significance for both comparisons ($p < 0.002$). It is interesting to notice that, despite the variability of the microbial consortia identified across the heights of the reactor, no differences were detected from a visual inspection of the generated biofilm. Moreover, microbial composition differences between corresponding sampling points of TBR1 and TBR2 were not significantly different. This suggests that the different pressure levels were not considerably affecting the composition of microbiomes. Therefore, the higher solubility of gasses induced in TBR2 did not select species for particular specific metabolic adaptation.

To obtain an optimal functional analysis, the problem of characterization based on incomplete annotation derived from fragmented MAG genomes had to be buffered. For this reason, the most relevant MAGs were compared with the Bio-Gas Microbiome database (see Supplementary Materials). High genetic similarity (i.e. Average Nucleotide Identity) is a solid proxy to identify MAGs belonging to the same species (Jain et al., 2018); therefore, the more complete MAG in each recovered cluster was used for further functional analysis. Additionally, the microbiome of a TBR fed with real biogas from a full-scale biogas plant was also included in the comparison (Tsapekos et al., 2021). Out of the 47 abundant MAGs (relative abundance > 1 % in at least one sample) of the current work, 30 have been detected to be present also in the TBR fed with real biogas (see Supplementary Materials) (Tsapekos et al., 2021). This result highlights that only a limited number of microbial species from the original inoculum are remaining and thrive in the TBRs. The detected differences between the current work and the previous experiment on the TBR can be ascribed to the biochemical composition of the feeding digestate (cattle manure vs municipal biowaste), that may have affected the availability of macro/micronutrients, and to the different system of operation. Specifically, the operational parameters were tuned to improve efficiency and also, avoid common operational problems, such as blocking of the gas flow. For instance, a completely different trickling strategy was applied in the present work compared to the study from literature. Herein, a continuous trickling was applied in parallel with regular flooding to ensure wetting of material and high abundance of nutrients. In contrast, limited trickling for once per day with no flooding was applied in the cited TBR. Thus, the availability of nutrients was markedly higher in the present work.

In the current microbiome the most abundant species was *Methanobacterium* DTU-pt_142, which was mainly associated with the bottom-middle part of both reactors, where the biomethane was mainly formed. This species demonstrated an irregular distribution across the different levels at long GRT, which became more uniform, even though relatively less abundant, at short GRT. Similarly, the observed reduction in relative abundance of DTU-pt_142 as a consequence of the GRT shortening was also detected for *Methanobacterium formicicum* after GRT reduction in ex-situ biogas upgrading reactors (Ghofrani-Isfahani et al., 2021). It is important to notice that the metagenomic investigation

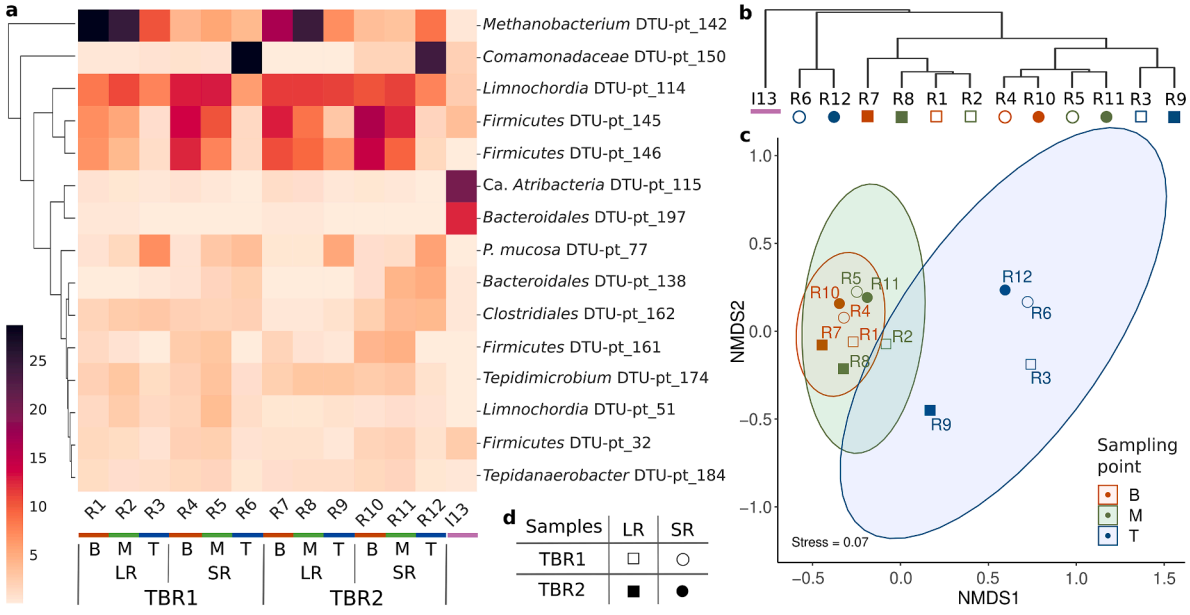

Fig. 5. Samples characterization according to abundance and distribution of recovered MAGs: a. Heatmap representing the relative abundance of the 15 most abundant MAGs. On the bottom of the figure samples are ordered according to the heights of the sampling point (Bottom, Middle, Top), the feeding regime (short - SR and long - LR GRT) and the corresponding TBR. b. Hierarchical clustering based on euclidean distances of microbial relative abundance between sampling points highlight similar abundance profiles. The different shapes of the symbols represent samples collected from the first (empty) or second (filled) reactor at a long (square) or short (circle) GRT c. NMDS plot based on Bray-Curtis distances between sampling points; 95% confidence ellipses were drawn for samples collected at different levels of the TBRs d. Summary table of the code used to mark the samples.

method has some limitations in providing absolute species abundance values in biological systems. Therefore, the described trends observed through changes in microbial relative abundance between sampling points may be also affected by undetected differences in the total microbial community size.

The functional inspection of DTU-pt_142 identified the presence of a complete hydrogenotrophic methane production pathway able to support autotrophic CO_2 assimilation for carbon fixation (Fig. 6a). Species belonging to the genus *Methanobacterium* sp. are known to be able to convert H_2 and CO_2 into CH_4 (Jee et al., 1988) and recently were detected as abundant in different biogas upgrading reactors (Gao et al., 2021). In the current system, DTU-pt_142 was the main methanogen and the most important microorganism for the upgrading process. The dominance of this archaeon can be explained with the hypothesis that during long-term organic carbon starvation, it upregulates the expression of essential genes involved in methanogenesis, such as hydrogenase B (ehb), carbon monoxide dehydrogenase, and acetyl-CoA decarbonylase/synthase (Zhu et al., 2020). The fine regulation provides important energetic competitive advantages as it has been suggested that Ehb instead of the other energy converting hydrogenase, present in *M. thermophilus*, was more effective when the growth was constrained to CO_2 as the sole carbon source (Zhu et al., 2020).

Moreover, the role of DTU-pt_142 probably did not limit to being the main hydrogenotrophic archaea in the community. In fact, even though in mesophilic conditions, *Methanobacterium* spp. have been previously demonstrated to be able to secrete extracellular polysaccharides (EPS), thus DTU-pt_142 was probably involved in biofilm formation (Veiga et al., 1997). The inspection of functional annotation highlighted that DTU-pt_142 had a set of genes related to capsular polysaccharide synthesis and sugar transfer (cpsG, cpsM, cpsO) (see Supplementary Materials) which are potentially involved in the generation of the EPS layer. Nevertheless, given the uniform distribution of biofilm across the TBR height, the formation of the extracellular matrix is probably attributable to more than a single species. In fact, the functional annotation identified other abundant bacterial species, such as *Comamonadaceae* DTU-pt_150 and *Firmicutes* DTU-pt_146, as putative responsible for the EPS formation.

Furthermore, bacteria showed a structured organization within the reactors. Some species, such as *Petrimonas mucosa* DTU-pt_77, *Bacillus* DTU-pt_91 and *Comamonadaceae* DTU-pt_150, presented different and complete oxidative pathways of the central carbon metabolism (Fig. 6a). Regarding *P. mucosa,* the inferred functional capacities were confirmed in a previous study that demonstrated its ability to grow using different carbohydrates under anaerobic condition (Hahnke et al., 2016). The

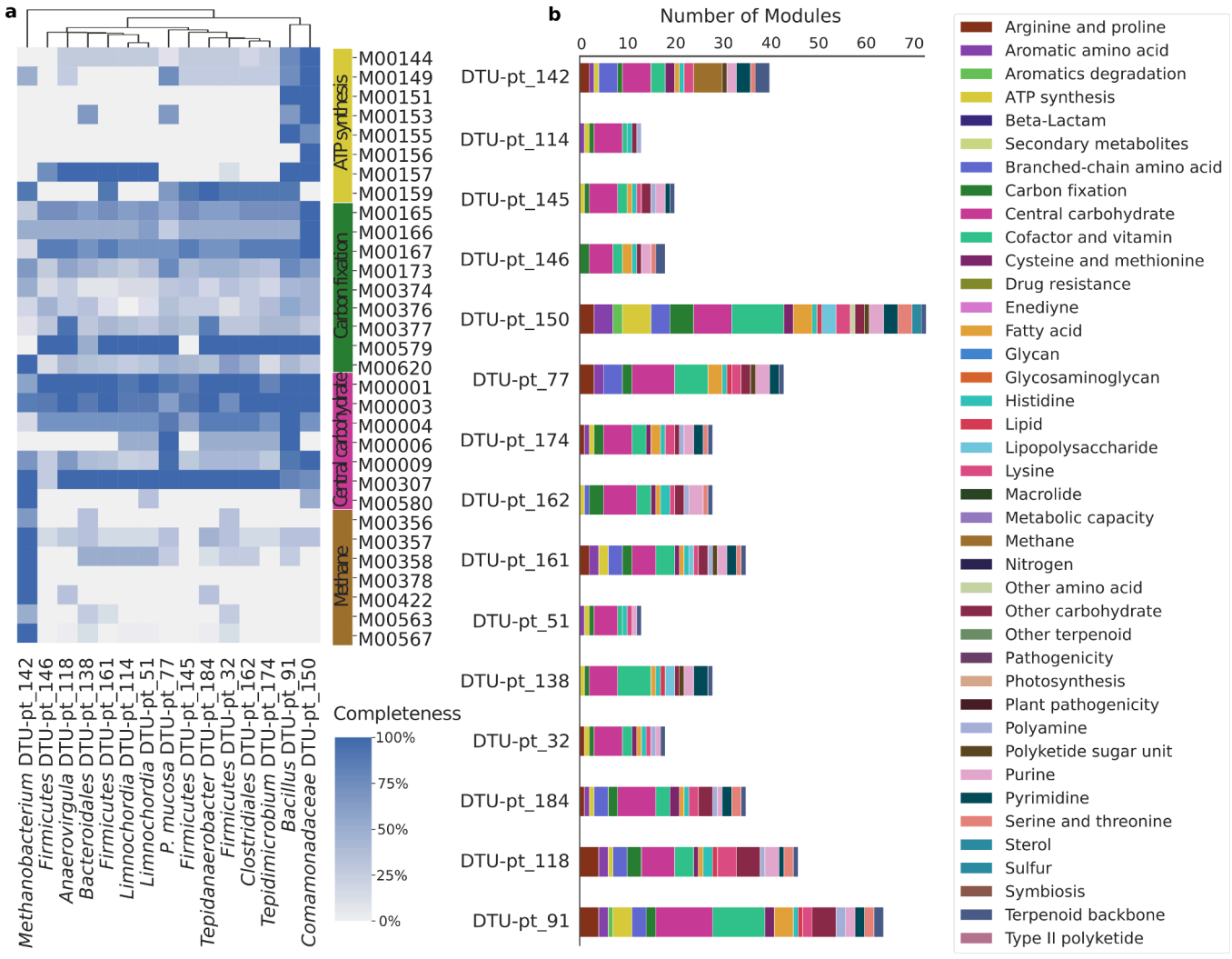

Fig. 6. Relevant pathway completeness and number of metabolic modules per category per genome of the most abundant MAGs. a. Heatmap representing completeness level of relevant KEGG modules reported as a percentage. Colored bars indicate the functional category of each metabolic pathway. b. Barplot of the number of modules with a completeness level higher than 80% per each MAG. Colors classify the metabolic category assigned to each module and MAGs were listed according to their average RA. Only MAGs with an average relative abundance higher than 1% are reported.

described metabolic capacities reflect the fact that these bacteria were detected in higher relative abundance in the upper layers, where some minor amount of residual carbohydrates was provided with the digestate. Thus, they prevailed close to the point where the digestate was trickling downwards for wetting and nutrients provision. On the contrary, other dominant species, such as *Limnochordia* DTU-pt_114, *Firmicutes* DTU-pt_145, and *Firmicutes* DTU-pt_146, showed a different distribution and were abundant in the bottom and middle layers of both reactors throughout the entire experiment. These three species presented similar metabolic pathways which may suggest redundant functional roles and a potentially competitive coexistence (see Supplementary Materials), however sophisticated mechanisms of interaction may justify their co-existence. Based on the comparison with the Bio-Gas Microbiome database DTU-pt_114, DTU-pt_145 and DTU-pt_146 have been previously identified in the TBR and in biofilm generated on the H_2 and CO_2 diffusers of four CSTR reactors for *ex-situ* biogas upgrading (De Bernardini et al., 2022). DTU-pt_114 (previous *Clostridiaceae* DTU-pt_99 or *Limnochordia* sp. GSMM975) has been suggested as homoacetogenic bacteria and facultative syntrophic of the species *Methanothermobacter wolfeii*. In the current TBR experiments, the abundance profile of DTU-pt_114 was co-occurring with that of *Methanobacterium* sp., suggesting that this bacterium is putatively capable of establishing facultative syntrophic interactions with more than one hydrogenotrophic archaea. Observing the functional annotation of DTU-pt_114, DTU-pt_145, DTU-pt_146 and the hypothetical syntrophic archaea an interesting pattern was highlighted. DTU-pt_142 presented a rich metabolism being able to synthesize many energetically demanding amino acids, whereas the bacteria lack any complete amino acids biosynthetic pathway (see Supplementary Materials). This result suggests that the bacteria may share a dependency towards *Methanobacterium* DTU-pt_142 and can help to explain the importance of this archaea within the community. In particular, the metabolic potential based on the genetic content highlighted the complementarity of histidine biosynthesis and degradation given that DTU-pt_142 has the complete pathway for its production whereas all bacteria seem to be able to process this amino acid for growing. Previous studies have already hypothesized the exchanges of amino acids to be fundamental in the establishment of cooperative communities (Machado et al., 2021). The high relative abundance of *Limnochordia* DTU-pt_114 (on average the second most abundant among all the samples – 10.56 % ± 2.26 %), confirmed that also this species generally plays a central role within the biofilm development in biogas reactors operating under thermophilic conditions. In fact, DTU-pt_114 and *Firmicutes*_DTU-pt_145 (previous *Firmicutes* sp. GSMM974) were two of the three microbes proposed to be responsible for biofilm formation, having genes involved in exopolysaccharides generation (De Bernardini et al., 2022) (see Supplementary Materials). However, in-depth understanding of the role that bacteria and archaeal species have on biofilm formation requires additional investigations of its development and structure. Further studies could monitor parameters, such as thickness and biochemical composition, in order to develop a model that correlates biofilm formation and microbial community stratification.

The analysis of the abundance profiles also highlighted *Comamonadaceae* DTU-pt_150, *Firmicutes* DTU-pt_161 and *Bacteroidales* DTU-pt_138 as bacteria having an intriguing role in the community. The increment in relative abundance of these species, especially DTU-pt_150, in both reactors under short GRT regime (e.g. R6 and R12) suggests a shared competitive advantage related to this operational parameter. Therefore, the most probable selective parameter influencing the microbiome is the higher gas feeding flux. In accordance, an experimental-modeling study showed that homo-acetogenic bacteria grow better than methanogenic archaea at alkaline pH and increased H_2 partial pressure (Tsapekos et al., 2022). Such a condition was established in the reactors due to the GRT reduction and the higher CO_2:H_2 feeding ratio in the feedstock. This hypothesis is further corroborated from the fact that DTU-pt_150, DTU-pt_161, and DTU-pt_138 were the only MAGs, among the 15 most abundant, that were not detected in the previous TBR study, which operated at much longer GRT (≥2h).

Given the relevant role of DTU-pt_150 in the community, the MAG was inspected to identify the origin of the metabolic advantage at short GRT. This species was the only abundant proteobacteria in the community; its genome was large (3,6 Mb) and showed, compared to the other MAGs, the highest number of metabolic modules (Fig. 6b). The functional annotation of this bacteria, together with those of DTU-pt_138 and DTU-pt_161, did not show a complete Wood–Ljungdahl Pathway or any other related pathway (e.g. Reductive Glycine Pathway and Glycine Synthase-Reductase Pathway) capable of sustaining the reduction of CO_2 and its fixation into biomass. Therefore, based on the fact that CO_2 was by far the most available carbon source in the system and that DTU-pt_150 has a very high relative abundance, it is only possible to hypothesize this MAG to be chemoautotrophs (i.e. able to fix and grow on CO_2). A further scrutinization of DTU-pt_150 metabolic potential suggested the possibility to consume acetate via an acetotrophic path (detected KO: K00925, K00625, K01895). Although the inference of behavior from genetic content may overlook many important biochemical mechanisms, this finding could provide an explanation for the observed acetate concentration drop (~758.65 mg/L) detected in both reactors between the first and second sampling points.

Overall the microbial spatial stratification within each reactor could be attributed, in addition to the higher concentrations of H_2 and CO_2 at the top of the reactor to the nutrient provision strategy (Tsapekos et al., 2021). Moreover, previous studies faced reactor clogging after only sixty days of operation due to poorly filtered medium (Sieborg et al., 2020) and uneven biofilm formation due to irregular trickling and no flooding of the reactor (Tsapekos et al., 2021). Thus, biofilm formation can be significantly affected by nutrients composition and content. In fact, a higher concentration of nutrients derived from the recirculating digestate was likely to be present in the top layers of the TRBs. This way of operating is probably the reason that facilitated the development of bacterial rich communities in the reactor upper layer that was exposed to the initial concentrations of gasses and liquid flows. Gasses and nutrients were gradually consumed downwards along the reactor column (see Supplementary Materials). Such environmental condition should have theoretically favored the enrichment of methanogenic archaea in the upper layers. In fact, hydrogenotrophic methanogenic activity and homo-acetogenic activity were previously found to be favored in close proximity with the H_2 supplementation area in membrane reactors (Garcia-Robledo et al., 2016). Nevertheless, in the current experiment, the relative abundance of *Methanobacterium* DTU-pt_142 was relatively higher in the bottom and middle layers. It is interesting to notice that the lower abundance did not imply metabolic inhibition of the archaea, in fact, Fig. 3 demonstrates that, at long GRT regimes, archaea in the upper points of the TBR were highly active and were responsible for a third of the methane yield. The same cannot be said when the reactors were operated at shorter GRT. In this case, even though the relative abundance of DTU-pt_142 was lower (on average 4.89 % ± 1.99 %) but homogeneous across the reactor (see Supplementary Materials), only the methanogenic communities located towards the bottom of the TBRs appeared extremely active. As a result, most of the CO_2 was fixed in the bottom-middle layers, as shown by monitoring the CH_4 evolution over TBR height. Overall, the observation of the time series of biogas composition over the TBR height demonstrated that the shortening of GRT caused the decrease of biomethanation efficiency in the upper layers.

4. Conclusions

This study demonstrated the effect of elevating pressure on the minimum achievable GRT maintaining high CH_4 content. The elevated pressure did not significantly affect the microbial composition, despite resulting in successful biomethanation at a short GRT due to the improved transfer rates of gases. Furthermore, metagenomic analysis

revealed that the microbial populations collected from the lower and middle parts of the TBRs under the same GRT were the most homogeneous, whereas those developed in the upper layer were relatively diverse. Overall, high CH_4 content (>90 %) can be achieved at GRT of 18 min, when shortage of nutrients is avoided.

CRediT authorship contribution statement

Farinaz Ebrahimian: Investigation, Data curation, Writing – original draft. **Nicola De Bernardini:** Software, Methodology, Data curation, Writing – original draft. **Panagiotis Tsapekos:** Conceptualization, Visualization, Investigation, Methodology, Writing – review & editing. **Laura Treu:** Funding acquisition, Resources, Conceptualization, Data curation, Supervision, Writing – review & editing. **Xinyu Zhu:** Investigation, Methodology, Data curation. **Stefano Campanaro:** Funding acquisition, Resources, Investigation, Writing – review & editing. **Keikhosro Karimi:** Supervision, Writing – review & editing. **Irini Angelidaki:** Funding acquisition, Resources, Conceptualization, Writing – review & editing.

Declaration of Competing Interest

The authors declare that they have no known competing financial interests or personal relationships that could have appeared to influence the work reported in this paper.

Data availability

Data will be made available on request.

Acknowledgements

This work was supported by the Danish EUDP under the project “eFuel-Electro fuel from a bio-trickling filter” (Project ID 64018-0559) and the LIFE Programme (LIFE20 CCM/GR/001642). The graphical abstract was created with BioRender.com.

Appendix A. Supplementary data

Supplementary data to this article can be found online at https://doi.org/10.1016/j.biortech.2022.127701.

References

Alneberg, J., Bjarnason, B.S., De Bruijn, I., Schirmer, M., Quick, J., Ijaz, U.Z., Lahti, L., Loman, N.J., Andersson, A.F., Quince, C., 2014. Binning metagenomic contigs by coverage and composition. Nat. Methods 11 (11), 1144–1146. https://doi.org/10.1038/nmeth.3103.

Ashraf, M.T., Sieborg, M.U., Yde, L., Rhee, C., Shin, S.G., Triolo, J.M., 2020. Biomethanation in a thermophilic biotrickling filter—pH control and lessons from long-term operation. Bioresour. Technol. Rep. 11, 100525 https://doi.org/10.1016/j.biteb.2020.100525.

Asimakopoulos, K., Łężyk, M., Grimalt-Alemany, A., Melas, A., Wen, Z., Gavala, H.N., Skiadas, I.V., 2020. Temperature effects on syngas biomethanation performed in a trickle bed reactor. Chem. Eng. J. 393, 124739 https://doi.org/10.1016/j.cej.2020.124739.

Asnicar, F., Thomas, A.M., Beghini, F., Mengoni, C., Manara, S., Manghi, P., Zhu, Q., Bolzan, M., Cumbo, F., May, U., 2020. Precise phylogenetic analysis of microbial isolates and genomes from metagenomes using PhyloPhlAn 3.0. Nat. Commun. 11 (1), 1–10.

Basile, A., Campanaro, S., Kovalovszki, A., Zampieri, G., Rossi, A., Angelidaki, I., Valle, G., Treu, L., 2020. Revealing metabolic mechanisms of interaction in the anaerobic digestion microbiome by flux balance analysis. Metab. Eng. 62, 138–149.

Bassani, I., Kougias, P.G., Angelidaki, I., 2016. In-situ biogas upgrading in thermophilic granular UASB reactor: key factors affecting the hydrogen mass transfer rate. Bioresour. Technol. 221, 485–491. https://doi.org/10.1016/j.biortech.2016.09.083.

Bolger, A.M., Lohse, M., Usadel, B., 2014. Trimmomatic: a flexible trimmer for Illumina sequence data. Bioinform. 30 (15), 2114–2120. https://doi.org/10.1093/bioinformatics/btu170.

Bowers, R.M., Kyrpides, N.C., Stepanauskas, R., Harmon-Smith, M., Doud, D., Reddy, T., Schulz, F., Jarett, J., Rivers, A.R., Eloe-Fadrosh, E.A., 2017. Minimum information about a single amplified genome (MISAG) and a metagenome-assembled genome (MIMAG) of bacteria and archaea. Nat. Biotechnol. 35 (8), 725–731. https://doi.org/10.1038/nbt.3893.

Braga Nan, L., Trably, E., Santa-Catalina, G., Bernet, N., Delgenès, J.-P., Escudié, R., 2020. Biomethanation processes: new insights on the effect of a high H_2 partial pressure on microbial communities. Biotechnol. Biofuels 13 (1), 1–17. https://doi.org/10.1186/s13068-020-01776-y.

Campanaro, S., Treu, L., Rodriguez-R, L.M., Kovalovszki, A., Ziels, R.M., Maus, I., Zhu, X., Kougias, P.G., Basile, A., Luo, G., 2020. New insights from the biogas microbiome by comprehensive genome-resolved metagenomics of nearly 1600 species originating from multiple anaerobic digesters. Biotechnol. Biofuels 13 (1), 1–18.

Chaumeil, P.-A., Mussig, A.J., Hugenholtz, P., Parks, D.H., 2020. GTDB-Tk: a toolkit to classify genomes with the Genome Taxonomy Database. Bioinform. https://doi.org/10.1093/bioinformatics/btz848.

De Bernardini, N., Basile, A., Zampieri, G., Kovalovszki, A., Diaz, B.D.D., Offer, E., Wongfaed, N., Angelidaki, I., Kougias, P.G., Campanaro, S., Treu, L., 2022. Integrating metagenomic binning with flux balance analysis to unravel syntrophies in anaerobic CO_2 methanation. Microbiome. https://doi.org/10.1186/s40168-022-01311-1.

Díaz, I., Fdz-Polanco, F., Mutsvene, B., Fdz-Polanco, M., 2020. Effect of operating pressure on direct biomethane production from carbon dioxide and exogenous hydrogen in the anaerobic digestion of sewage sludge. Appl. Energy 280, 115915.

Dupnock, T.L., Deshusses, M.A., 2017. High-performance biogas upgrading using a biotrickling filter and hydrogenotrophic methanogens. Appl. Biochem. Biotechnol. 183 (2), 488–502. https://doi.org/10.1007/s12010-017-2569-2.

Dupnock, T.L., Deshusses, M.A., 2021. Development and validation of a comprehensive model for biotrickling filters upgrading biogas. Chem. Eng. J. 407, 126614.

Fontana, A., Kougias, P.G., Treu, L., Kovalovszki, A., Valle, G., Cappa, F., Morelli, L., Angelidaki, I., Campanaro, S., 2018. Microbial activity response to hydrogen injection in thermophilic anaerobic digesters revealed by genome-centric metatranscriptomics. Microbiome 6 (1), 1–14. https://doi.org/10.1186/s40168-018-0583-4.

Gao, T., Zhang, H., Xu, X., Teng, J., 2021. Mutual effects of CO_2 absorption and H_2-mediated electromethanogenesis triggering efficient biogas upgrading. Sci. Total Environ. 151732 https://doi.org/10.1016/j.scitotenv.2021.151732.

Garcia-Robledo, E., Ottosen, L.D., Voigt, N.V., Kofoed, M., Revsbech, N.P., 2016. Micro-scale H_2–CO_2 dynamics in a hydrogenotrophic methanogenic membrane reactor. Front. Microbiol. 7, 1276. https://doi.org/10.3389/fmicb.2016.01276.

Ghofrani-Isfahani, P., Tsapekos, P., Peprah, M., Kougias, P., Zhu, X., Kovalovszki, A., Zervas, A., Zha, X., Jacobsen, C.S., Angelidaki, I., 2021. Ex-situ biogas upgrading in thermophilic up-flow reactors: the effect of different gas diffusers and gas retention times. Bioresour. Technol. 340, 125694 https://doi.org/10.1016/j.biortech.2021.125694.

Hahnke, S., Langer, T., Koeck, D.E., Klocke, M., 2016. Description of Proteiniphilum saccharofermentans sp. nov., Petrimonas mucosa sp. nov. and Fermentimonas caenicola gen. nov., sp. nov., isolated from mesophilic laboratory-scale biogas reactors, and emended description of the genus Proteiniphilum. Int. J. Syst. Evol. Microbiol. 66 (3), 1466–1475.

Huerta-Cepas, J., Szklarczyk, D., Heller, D., Hernández-Plaza, A., Forslund, S.K., Cook, H., Mende, D.R., Letunic, I., Rattei, T., Jensen, L.J., 2019. eggNOG 5.0: a hierarchical, functionally and phylogenetically annotated orthology resource based on 5090 organisms and 2502 viruses. Nucleic Acids Res. 47 (D1), D309–D314. https://doi.org/10.1093/nar/gky1085.

Hyatt, D., Chen, G.-L., LoCascio, P.F., Land, M.L., Larimer, F.W., Hauser, L.J., 2010. Prodigal: prokaryotic gene recognition and translation initiation site identification. BMC Bioinform. 11 (1), 1–11. https://doi.org/10.1186/1471-2105-11-119.

Inkeri, E., Tynjälä, T., 2020. Modeling of CO_2 capture with water bubble column reactor. Energies 13 (21), 5793. https://doi.org/10.3390/en13215793.

Jain, C., Rodriguez-R, L.M., Phillippy, A.M., Konstantinidis, K.T., Aluru, S., 2018. High throughput ANI analysis of 90K prokaryotic genomes reveals clear species boundaries. Nat. Commun. 9 (1), 1–8. https://doi.org/10.1038/s41467-018-07641-9.

Jee, H.S., Nishio, N., Nagai, S., 1988. Continuous CH_4 Production from H_2 and CO_2 by Methanobacterium thermoautotrophicum in a fixed-bed reactor. J. Fermentation Technol. 66 (2), 235–238. https://doi.org/10.1016/0385-6380(88)90054-4.

Jønson, B.D., Sieborg, M.U., Ashraf, M.T., Yde, L., Shin, J., Shin, S.G., Triolo, J.M., 2020. Direct inoculation of a biotrickling filter for hydrogenotrophic methanogenesis. Bioresour. Technol. 318, 124098 https://doi.org/10.1016/j.biortech.2020.124098.

Kang, D.D., Froula, J., Egan, R., Wang, Z., 2015. MetaBAT, an efficient tool for accurately reconstructing single genomes from complex microbial communities. PeerJ 3, e1165.

Kang, D.D., Li, F., Kirton, E., Thomas, A., Egan, R., An, H., Wang, Z., 2019. MetaBAT 2: an adaptive binning algorithm for robust and efficient genome reconstruction from metagenome assemblies. PeerJ 7, e7359.

Kougias, P., Tsapekos, P., Treu, L., Kostoula, M., Campanaro, S., Lyberatos, G., Angelidaki, I., 2020. Biological CO_2 fixation in up-flow reactors via exogenous H_2 addition. J. Biotechnol. 319, 1–7. https://doi.org/10.1016/j.jbiotec.2020.05.012.

Letunic, I., Bork, P., 2021. Interactive Tree Of Life (iTOL) v5: an online tool for phylogenetic tree display and annotation. Nucleic Acids Res. 49 (W1), W293–W296.

Li, D., Liu, C.-M., Luo, R., Sadakane, K., Lam, T.-W., 2015. MEGAHIT: an ultra-fast single-node solution for large and complex metagenomics assembly via succinct de Bruijn graph. Bioinform. 31 (10), 1674–1676. https://doi.org/10.1093/bioinformatics/btv033.

Liu, R., Hao, X., Wei, J., 2016. Function of homoacetogenesis on the heterotrophic methane production with exogenous H_2/CO_2 involved. Chem. Eng. J. 284, 1196–1203.

Machado, D., Maistrenko, O.M., Andrejev, S., Kim, Y., Bork, P., Patil, K.R., Patil, K.R., 2021. Polarization of microbial communities between competitive and cooperative metabolism. Nat. Ecol. Evol. 5 (2), 195–203. https://doi.org/10.1038/s41559-020-01353-4.

Martin, M.R., Fornero, J.J., Stark, R., Mets, L., Angenent, L.T., 2013. A single-culture bioprocess of Methanothermobacter thermautotrophicus to upgrade digester biogas by CO_2-to-CH_4 conversion with H_2. Archaea 2013. https://doi.org/10.1155/2013/157529.

Mauerhofer, L.-M., Zwirtmayr, S., Pappenreiter, P., Bernacchi, S., Seifert, A.H., Reischl, B., Schmider, T., Taubner, R.-S., Paulik, C., Simon, K.-M.-R., 2021. Hyperthermophilic methanogenic archaea act as high-pressure CH_4 cell factories. Commun. Biol. 4 (1), 1–12.

Merkle, W., Baer, K., Lindner, J., Zielonka, S., Ortloff, F., Graf, F., Kolb, T., Jungbluth, T., Lemmer, A., 2017. Influence of pressures up to 50 bar on two-stage anaerobic digestion. Bioresour. Technol. 232, 72–78. https://doi.org/10.1016/j.biortech.2017.02.013.

Nissen, J.N., Johansen, J., Allesøe, R.L., Sønderby, C.K., Armenteros, J.J.A., Grønbech, C. H., Jensen, L.J., Nielsen, H.B., Petersen, T.N., Winther, O., 2021. Improved metagenome binning and assembly using deep variational autoencoders. Nat. Biotechnol. 39 (5), 555–560.

Porté, H., Kougias, P.G., Alfaro, N., Treu, L., Campanaro, S., Angelidaki, I., 2019. Process performance and microbial community structure in thermophilic trickling biofilter reactors for biogas upgrading. Sci. Total Environ. 655, 529–538.

Pruesse, E., Peplies, J., Glöckner, F.O., 2012. SINA: accurate high-throughput multiple sequence alignment of ribosomal RNA genes. Bioinform. 28 (14), 1823–1829.

Ruiz-Perez, C.A., Conrad, R.E., Konstantinidis, K.T., 2021. MicrobeAnnotator: a user-friendly, comprehensive functional annotation pipeline for microbial genomes. BMC Bioinform. 22 (1), 1–16. https://doi.org/10.1186/s12859-020-03940-5.

Sieborg, M.U., Jønson, B.D., Ashraf, M.T., Yde, L., Triolo, J.M., 2020. Biomethanation in a thermophilic biotrickling filter using cattle manure as nutrient media. Bioresour. Technol. Rep. 9, 100391 https://doi.org/10.1016/j.biteb.2020.100391.

Thema, M., Weidlich, T., Kaul, A., Böllmann, A., Huber, H., Bellack, A., Karl, J., Sterner, M., 2021. Optimized biological CO_2-methanation with a pure culture of thermophilic methanogenic archaea in a trickle-bed reactor. Bioresour. Technol. 333, 125135.

Treu, L., Kougias, P., de Diego-Díaz, B., Campanaro, S., Bassani, I., Fernández-Rodríguez, J., Angelidaki, I., 2018. Two-year microbial adaptation during hydrogen-mediated biogas upgrading process in a serial reactor configuration. Bioresour. Technol. 264, 140–147.

Treu, L., Tsapekos, P., Peprah, M., Campanaro, S., Giacomini, A., Corich, V., Kougias, P. G., Angelidaki, I., 2019. Microbial profiling during anaerobic digestion of cheese whey in reactors operated at different conditions. Bioresour. Technol. 275, 375–385.

Tsapekos, P., Alvarado-Morales, M., Angelidaki, I.J.J.o.E.C.E., 2022. H_2 competition between homoacetogenic bacteria and methanogenic archaea during biomethanation from a combined experimental-modelling approach. J. Environ. Chem. Eng., 107281.

Tsapekos, P., Treu, L., Campanaro, S., Centurion, V.B., Zhu, X., Peprah, M., Zhang, Z., Kougias, P.G., Angelidaki, I., 2021. Pilot-scale biomethanation in a trickle bed reactor: process performance and microbiome functional reconstruction. Energy Convers. Manag. 244, 114491 https://doi.org/10.1016/j.enconman.2021.114491.

Ullrich, T., Lindner, J., Bär, K., Mörs, F., Graf, F., Lemmer, A., 2018. Influence of operating pressure on the biological hydrogen methanation in trickle-bed reactors. Bioresour. Technol. 247, 7–13. https://doi.org/10.1016/j.biortech.2017.09.069.

Veiga, M.C., Jain, M.K., Wu, W., Hollingsworth, R.I., Zeikus, J.G., 1997. Composition and role of extracellular polymers in methanogenic granules. Appl. Environ. Microbiol. 63 (2), 403–407. https://doi.org/10.1128/aem.63.2.403-407.1997.

Wu, Y.-W., Tang, Y.-H., Tringe, S.G., Simmons, B.A., Singer, S.W., 2014. MaxBin: an automated binning method to recover individual genomes from metagenomes using an expectation-maximization algorithm. Microbiome 2 (1), 1–18.

Zhu, X., Campanaro, S., Treu, L., Seshadri, R., Ivanova, N., Kougias, P.G., Kyrpides, N., Angelidaki, I., 2020. Metabolic dependencies govern microbial syntrophies during methanogenesis in an anaerobic digestion ecosystem. Microbiome 8 (1), 1–14.